

Scar functions in the Bunimovich Stadium billiard.

Gabriel G. Carlo⁽¹⁾, Eduardo G. Vergini⁽²⁾
and Pablo Lustemberg⁽²⁾

(1)Max-Planck-Institut für Physik komplexer Systeme,
Nöthnitzer Str. 38, D-01187 Dresden, Germany.

(2)Departamento de Física, Comisión Nacional de
Energía Atómica. Av. del Libertador 8250,
1429 Buenos Aires, Argentina.

February 8, 2008

Abstract

In the context of the semiclassical theory of short periodic orbits, scar functions play a crucial role. These wavefunctions live in the neighbourhood of the trajectories, resembling the hyperbolic structure of the phase space in their immediate vicinity. This property makes them extremely suitable for investigating chaotic eigenfunctions. On the other hand, for all practical purposes reductions to Poincaré sections become essential. Here we give a detailed explanation of resonances and scar functions construction in the Bunimovich stadium billiard and the corresponding reduction to the boundary. Moreover, we develop a method that takes into account the departure of the unstable and stable manifolds from the linear regime. This new feature extends the validity of the expressions.

PACS:05.45.Mt, 03.65.Sq, 45.05.+x

1 Introduction

During the past few years, research carried out on chaotic eigenfunctions has provided very important results. Berry and Voros [1, 2] conjectured that, in the semiclassical limit, these eigenfunctions would be locally like random superpositions of plane waves; this conjecture is supported by theorems of Shnirelman [3] and Colin de Verdière [4]. But Heller [5] found that a large number of highly excited eigenfunctions of the Bunimovich stadium billiard [6] have density enhancements along the shortest periodic orbits (**POs**). Since then several studies have focused on these phenomena and led to theoretical developments [7] and experimental observations such as in macroscopic billiard-shaped microwave cavities [8], tunnel junctions [9] and Hydrogen atoms in strong magnetic fields [10, 11].

Recently, a variety of new approaches to study the structure of chaotic eigenfunctions have been developed [12, 13, 14, 15]. One of them consists of the semiclassical construction of resonances with hyperbolic structure associated to unstable periodic orbits [15]. These resonances were studied both analytically and numerically. They are classically motivated constructions that take into account complete classical information in the neighbourhood of a **PO**. The so-called scar functions, as they have been named, can be obtained by a linear combination of resonances [16, 17] of a periodic orbit at a given energy with minimum energy dispersion. Resonances span a basis and are obtained by applying a creation operator over a vacuum state. The vacuum state (i.e. a resonance with no transverse excitations) is constructed with a (conveniently selected) Gaussian wave packet that follows a modified transverse motion along the chosen orbit. The modified motion, which is the result of dropping the pure hyperbolic one, describes a bunch of **POs** surrounding the chosen trajectory. For instance, the eigenvectors of the monodromy matrix evolve without the exponential contraction-dilation that is expected in this kind of hyperbolic dynamics. Instead, after one period they return to themselves (up to a minus sign in some cases). In the same way, the wave packet returns to itself with an accumulated phase that is an integral multiple of 2π , guaranteeing its continuity.

Billiards are among the most interesting and well-studied systems in quantum chaos. We are going to work with the Bunimovich stadium billiard. For billiards, the boundary is the natural Poincaré section. We present a formulation of resonances and scar functions over the boundary. This reduction makes the calculations easier and it is a clear advantage when exploring a great number of eigenfunctions. Of course this is not the only reason to obtain these scar functions expressions, since they are more than tools for investigating numerically the structure of chaotic eigenfunctions. They are the cornerstone of the semiclassical theory of short periodic orbits of References [16, 17]. In this context it is possible to obtain all quantum information of a chaotic Hamiltonian system just by knowing classical information of a small number of short **POs** (in fact, the shortest ones, whose number increases at most linearly with a Heisem-

berg time). This is accomplished by evaluating the interaction between **POs**. In previous calculations [17] only vacuum states of a handful of the shortest **POs** were used. For higher energies it is necessary to incorporate excitations to these vacuum states and also longer **POs**. All this can be done by using scar functions associated to a greater number of **POs** than the ones needed at low energy values. It is evident that working on the billiard domain will not be the best choice in these cases, and expressions on the boundary become essential. Hence, we need to develop an efficient method to evaluate them, this being one of the main goals of this article.

We also go further by taking into account the non linear behaviour of the unstable and stable manifolds. Then, we are able to extend the validity of scar functions beyond the linear regime. The chosen approach is general in nature, and despite it is applied to the special case of the Bunimovich stadium it can be extended to general systems in a straight forward way. These new ingredients do not significantly alter the construction of scar functions, which preserve their compact character. These new expressions provide a more comprehensive description of the phase space in the neighbourhood of each orbit. They are the other main goal of the present work.

This paper is organised as follows, Section 2 consists of a detailed explanation of the construction of resonances on the billiard domain. Here we address many subtleties involved in the wave function calculations and local expressions are provided. Moreover, a comprehensive approach is offered for resonances including vacuum states and excitations in a single formulation. Though the construction may seem complex the great advantage is that it is a general one, suitable for any billiard. In Section 3 the construction is extended with expressions on the boundary. In this part explicit formulas amenable to extensive and high energies calculations are presented. Also a brief summary of the results from the previous section and their application to the construction of scar functions on the billiard boundary is developed; here, we give explicit examples. Finally, Section 4 is devoted to conclusions.

2 Resonances on the billiard domain

In this section we give a thorough explanation of the construction of the resonances associated to a given trajectory γ of length L belonging to the Bunimovich stadium. We define a coordinate x along the trajectory and a coordinate y perpendicular to it (such that $y = 0$ defines the orbit). The evolution of an initial displacement (y, p_y) at $x = 0$ into $(y(x), p_y(x))$ at x can be obtained by means of the symplectic stability matrix $M(x)$ with elements m_{ij} ,

$$\begin{pmatrix} y(x) \\ p_y(x) \end{pmatrix} = \begin{pmatrix} m_{11}(x) & m_{12}(x) \\ m_{21}(x) & m_{22}(x) \end{pmatrix} \begin{pmatrix} y \\ p_y \end{pmatrix}.$$

The eigenvectors ξ_u and ξ_s of M give the unstable and stable directions associated to the orbit. These vectors evolve as $\tilde{\xi}_u(x) = M(x) \xi_u$. After one period they return over themselves, $\tilde{\xi}_u(L) = (-1)^\mu e^{\lambda L} \xi_u$ and $\tilde{\xi}_s(L) = (-1)^\mu e^{-\lambda L} \xi_s$, where μ is the total number of half turns made by $\tilde{\xi}_u(x)$ and $\tilde{\xi}_s(x)$ during its evolution along the orbit. For a billiard this number corresponds to $\mu = \nu + N_{ref}$ where ν is the maximum number of conjugated points (in particular, for the stadium ν is exactly the number of bounces with the circle). N_{ref} is the total number of reflections with the billiard boundary and the symmetry lines. This point will be addressed later when we refer to quantisation conditions.

We are going to decompose the motion given by $M(x)$ into a purely hyperbolic and a periodic one. In order to do so we need to specify the contraction-dilation rate along the manifolds. This can be done by first finding one of the x_0 points on the trajectory where the projections of $\xi_u(x_0)$ and $\xi_s(x_0)$ on y and p_y are equal in absolute value, i.e., the unstable and stable directions would be symmetrical with respect to the axes. There are 2ν points like these on the orbit. They can be found by using the fact that M_{x_0} (the return map starting at $x = x_0$) has equal diagonal elements when this condition on the eigenvectors is met. By means of the relation $M_{x_0} = M(x_0)M(L)M(x_0)^{-1}$ this condition can be easily implemented.

Then, we decompose $M(x)$ into a periodic matrix $F(x)$ describing the evolution of the manifolds and a matrix which is responsible of the contraction-dilation along them. This is just an application of Floquet theorem [18]:

$$M(x) = F(x) \exp[f(x) \lambda K], \quad (1)$$

where $K \equiv BDB^{-1}$ with D a diagonal matrix of elements $d_{11} = 1$ and $d_{22} = -1$ and $B = (\xi_u \ \xi_s)$, i.e., the symplectic matrix transforming coordinates from the new axes ξ_u and ξ_s to the old ones y and p_y . The real function $f(x)$ (required to fulfill $f(0) = 0$ and $f(L) = L$) can be seen as the relation between the lengths of $\tilde{\xi}_u(x)$ and ξ_u , but the plane y - p_y has no defined norm so establishing this relation is in general impossible. Further conditions can be imposed on $f(x)$, (see Ref. [15]). However, without loss of generality, we are going to consider the easier choice $f(x) = x$ for the present calculations. On the other hand the neutral motion given by $F(x)$ can be obtained by its action on ξ_u and ξ_s , allowing us to define the set $y_u(x)$, $y_s(x)$, $p_u(x)$ and $p_s(x)$ of periodic functions:

$$\begin{pmatrix} y_u(x) \\ p_u(x) \end{pmatrix} \equiv \xi_u(x) \equiv F(x) \xi_u = e^{-f(x)\lambda} M(x) \xi_u, \quad (2)$$

and

$$\begin{pmatrix} y_s(x) \\ p_s(x) \end{pmatrix} \equiv \xi_s(x) \equiv F(x) \xi_s = e^{f(x)\lambda} M(x) \xi_s. \quad (3)$$

Since $F(x)$ is area preserving, these functions satisfy the symplectic property $y_u(x)p_s(x) - y_s(x)p_u(x) = \xi_u(x) \wedge \xi_s(x) = \xi_u \wedge \xi_s = J$ (J being the unit of action in the y - p_y plane).

A resonance can be essentially seen as the product of a plane wave in the x direction, being the semiclassical approximation for the unidimensional motion along the orbit, and a Gaussian wave packet in the transverse coordinate, which follows a dynamics without dilation-contraction along the unstable and stable manifolds of the trajectory. The vacuum state (semiclassically normalised to unity) is given by [15]:

$$\psi_\gamma^{(0)}(x, y) = \frac{\exp\{i [S(x) + y^2 \Gamma(x)/2]/\hbar - i \phi(x)/2\}}{\sqrt{T} \dot{x} [\pi (\hbar/J) |Q(x)|^2]^{1/4}}, \quad (4)$$

where T is the period of the orbit and $\phi(x)$ is the angle swept by $Q(x)$ while evolving from 0 to x . In this expression $\Gamma(x) = P(x)/Q(x)$, where $Q(x)$ and $P(x)$ are the components of a complex vector constructed with the stable and unstable manifolds. These components are obtained as:

$$\begin{pmatrix} Q(x) = y_u(x) + i y_s(x) \\ P(x) = p_u(x) + i p_s(x) \end{pmatrix} \equiv \xi_u(x) + i \xi_s(x) = M(x) B \begin{pmatrix} e^{-f(x)\lambda} \\ i e^{f(x)\lambda} \end{pmatrix}. \quad (5)$$

For billiards we take a slightly modified evolution matrix ($\tilde{M}(x)$) in order to have a continuous $Q(x)$; since the phase $\phi(x)$ of $Q(x)$ must be known in detail for resonances construction, continuity is a very reasonable condition to ask for. This can be done by means of $\tilde{M}(x) \equiv (-1)^{N(x)} M(x)$, with $N(x)$ being the number of reflections while evolving from 0 to x . In turn, this matrix can be constructed by using two types of matrices:

$$M_1(l) = \begin{pmatrix} 1 & l \\ 0 & 1 \end{pmatrix}, \text{ and } M_2(\theta) = \begin{pmatrix} 1 & 0 \\ -2/\cos(\theta) & 1 \end{pmatrix}.$$

$M_1(l)$ describes the evolution for a path of length l without bounces with the circle (the transverse momentum is measured in units of the momentum along the trajectory). $M_2(\theta)$ takes into account a bounce with the circle (θ defines the angle between the incoming trajectory and the radial direction). In the following we assume this matrix instead of the original one given for the most general expressions in the previous theoretical introduction. The reflections related phase will be included in the expressions directly.

Taking the wave functions defined in Eq (4) as the vacuum state for appropriate creation-annihilation operators (see [15]), the following expression results for a resonance with m transverse excitations:

$$\psi_\gamma^{(m)}(x, y) = \frac{e^{-im\phi(x)}}{\sqrt{2^m m!}} H_m \left[\frac{y\sqrt{J/\hbar}}{|Q(x)|} \right] \psi_\gamma^{(0)}(x, y), \quad (6)$$

where $\phi(x)$ is the phase introduced in Eq (4), and $H_m(z)$ are the Hermite polynomials ($H_0 = 1$, $H_1 = 2\xi$, $H_2 = 4\xi^2 - 2$, ...). It is easy to see that $\psi_\gamma^{(m)}$ is also a product of two functions; the solution for the motion along the orbit and

m excitations of a transverse Gaussian wave packet which evolves following the same periodic motion previously mentioned.

Inside each family, resonances are identified by the integer number $n = 0, 1, \dots$, the number of excitations along the orbit and by $m = 0, 1, \dots$, the transverse excitations. The wave number k depends on γ , n and m through the rule:

$$S(L)/\hbar - N_b\pi/2 - (m + 1/2)\mu\pi = 2\pi n, \quad (7)$$

which guarantees the continuity of $\psi_\gamma^{(m)}$ at $x = L = 0$. In this expression $S(L) = \int_0^L p_x dx$ is the dynamical action and μ is the topological phase; that is, the number of half turns made by the manifolds along the orbit. Finally, N_b is a pure quantum phase related to the boundary conditions (see [15]), which is equal to the number of reflections satisfying Dirichlet boundary conditions minus the number of reflections satisfying Neumann conditions.

Rule (7) can be divided into the $m\mu$ even and odd cases:

$$S(L)/\hbar - N_b\pi/2 - \mu\pi/2 = 2\pi (n + m\mu/2) \quad (8)$$

for $m\mu$ even, and

$$S(L)/\hbar - N_b\pi/2 - 3\mu\pi/2 = 2\pi [n + (m-1)\mu/2], \quad (9)$$

for the odd case. For the desymmetrized stadium billiard it results in

$$S(L)/\hbar = Lk ; N_b = N_s + s_h N_h + s_v N_v$$

and $\mu = N_{ref} + \nu$ with $N_{ref} = N_s + N_h + N_v$ where N_s , N_h and N_v are the number of reflections with the stadium boundary and the horizontal and vertical symmetry lines respectively. Finally, ν is the number of bounces with the quarter of the circle. The value of s_h is 0 or 1 depending on the symmetry with respect to the horizontal axis being even or odd; this is equivalent for s_v , where the vertical symmetry is considered. The set of allowed m values can range from 0 or 1 (depending on $m\mu$ being even or odd) to $m < A_{eff}/2\pi\hbar$ (where A_{eff} is the transverse area in which the construction is valid). For simplicity, we are going to consider $0(1) \leq m < n$ as a satisfactory criterion.

The time reversal properties of the system under study can be applied to Eq (6), giving a real resonance expression. Resonances are constructed explicitly for the stadium billiard by assigning a semiclassical expression to each straight line of the orbit. The first one of these lines is the segment of γ that begins in $x_1 = 0$. Let $x_2 (> x_1)$ be the value of x where the path reaches the border of the stadium after the corresponding evolution. The path departing from x_2 defines the second line and so on until $x = L/2$ is reached. If we define local coordinates $(x^{(j)}, y^{(j)})$ over each line in such a way that $x^{(j)} = x$ inside the desymmetrized billiard, the expression for the j th line turns out to be [we

are going to use (x, y) in the following expressions, understanding that they represent the variables $(x^{(j)}, y^{(j)})$ of the j th line]

$$\begin{aligned} \psi_j^{(m)}(x, y) &= \left(\frac{kR}{|Q(x)|^2} \right)^{1/4} f^{(m)} \left[\frac{\sqrt{kR}y}{|Q(x)|} \right] \\ &\quad \frac{2}{\sqrt{L}} \sin[ky^2 g_j(x) + kx - N_b(x_j^+) \pi/2 - \\ &\quad -(m + 1/2)\Phi_j(x) - F_0 - mG_0]. \end{aligned} \quad (10)$$

Here $N_b(x_j^+)$ is defined in the same way as N_b but taking account of the bounces up to the point x_j (including it), the corresponding term takes into account the quantum phase associated to boundary conditions and this is the resonance counterpart of the phase considered in the quantisation conditions. Furthermore,

$$g_j(x) \equiv \text{Re}[\Gamma(x)/2] = \frac{y_u p_u + y_s p_s}{2(y_u^2 + y_s^2)}, \quad (11)$$

where the x dependence is understood. We would like to point out that the factor k in the term $ky^2 g_j(x)$ in Eq (10) is different from the factor $1/\hbar$ in Eq (4). This is due to the fact that momenta in the expression for $g_j(x)$ are measured in units of $\hbar k$, i.e., the momentum along the trajectory. The oscillator functions are defined by

$$f^{(m)}(\xi) = \pi^{-1/4} (2^m m!)^{-1/2} e^{-\xi^2/2} H_m(\xi),$$

where H_m is the m th degree Hermite polynomial. The *sine* function in Eq (10) was chosen in order to obtain real resonances by virtue of the time reversal symmetry of the system. We have taken $T\dot{x} = L$ in Eq (4) and considered $J = \hbar k R$ in Eq (6), with k the wave number from the quantisation conditions and R the circle radius of the stadium. Finally $\Phi_j(x) = N_{ref}(x_j^+) \pi + [\tilde{\varphi}_j + \phi_j(x) + \alpha_j(x)]$, with $\tilde{\varphi}_j = \tilde{\varphi}_{j-1} + \phi_{j-1}(x_j) + \alpha_{j-1}(x_j)$ for $j \geq 2$ and $\tilde{\varphi}_1 = 0$, follows the actual phase of $Q(x)$. In the first term of this expression we introduce the jumps in the sign of $Q(x)$ due to reflections on hard walls, that were avoided by using the $\tilde{M}(x)$ matrix instead of the right one. In fact, this is the only place where this change is needed because Γ keeps its sign. The remaining term of this function, i.e., $\tilde{\varphi}_j + \phi_j(x) + \alpha_j(x)$ is explained in the subsection 2.1.

The initial phase of the resonances $\psi_j^{(m)}$, Eq (10), is essential to satisfy the boundary conditions. We have set $\tilde{\varphi}_1 = 0$ in the relations that define $\tilde{\varphi}_j$, and account for the initial phase by means of two quantities, F_0 and G_0 , which take values as shown in Fig. 1. F_0 accounts for the initial phase in order to obtain an even (odd) function when symmetry is even (odd), without considering the symmetry of the oscillator functions (this will be addressed by G_0). In the case of having only one path to consider at the initial bounce, like in the first diagrams for both rows, the corresponding function must obey the symmetry

by itself. In the second case of the first row the symmetry related path is added but multiplied by -1 (see the final sum in this section and explanation thereby). Finally, in the two remaining cases (of the second row) an even function is needed since the function obtained by adding the symmetry related path multiplied by -1 (1) is (anti)symmetric. G_0 takes into account the symmetry of the Hermite polynomials, which goes like m , the number of transverse excitations. Its value depend on the starting angle of the trajectory. If this angle is zero, the symmetry of the resonance is the one given by the F_0 choice. In the other case, the symmetry of the oscillator function (i.e. Hermite polynomials) comes into play and in order to have the right final result we need to consider it. This can be easily accomplished by the choice of the G_0 value according to Fig. 1.

$$F_0 \begin{cases} 0 & \downarrow & \swarrow \\ \pi/2 & \downarrow & \swarrow & \swarrow \end{cases}$$

$$G_0 \begin{cases} 0 & \downarrow & \downarrow \\ \pi/2 & \swarrow & \swarrow & \swarrow \end{cases}$$

Figure 1: F_0 and G_0 values depending on the type of starting point and on the boundary conditions. Dashed (solid) lines correspond to the symmetrical (antisymmetrical) condition, i.e., $s_h, s_v = 0(1)$. Finally, arrows stand for the trajectories.

The transformation of local coordinates $(x^{(j)}, y^{(j)})$ over the j line to (X, Y) coordinates that belong to the horizontal and vertical directions respectively, can be obtained in a simple way by means of an usual transformation. If (X_j, Y_j) are the coordinates of the point x_j , and α_j is the angle between the j line and the horizontal direction, $(x^{(j)} - x_j, y^{(j)}) = G_j(X, Y)$ is given by

$$G_j(X, Y) = (X - X_j, Y - Y_j) \begin{pmatrix} \cos(\alpha_j) & -\sin(\alpha_j) \\ \sin(\alpha_j) & \cos(\alpha_j) \end{pmatrix}.$$

Finally, the family of resonances ψ_γ is constructed by means of all the lines including symmetries (see Fig. 2 where this procedure is illustrated for one of the shortest periodic orbits of the stadium billiard), this avoids unnecessary evaluation of reflection points over the symmetry lines, considering only those over the boundary:

$$\psi_\gamma(X, Y) = \sum_j \sum_{i=1}^{m_h} \sum_{l=1}^{m_v} h_i v_l \psi_j[(x_j, 0) + G_j(s_l X, s_i Y)]. \quad (12)$$

where $s_i \equiv (-1)^{i+1}$ and $s_l \equiv (-1)^{l+1}$. $h_i = [\delta_{i,1} + \delta_{i,2}(1 - 2s_h)]$ and $v_l = [\delta_{l,1} + \delta_{l,2}(1 - 2s_v)]$. m_h and m_v depend on j and are specified like this: $m_h = 1$ or 2 if the line is symmetrical or not with respect to the horizontal axis respectively, and the same happens with the number m_v for the vertical axis, although $m_h = 2$ and $m_v = 1$ if the line goes through the origin. This is the only considered choice of the two possible ones (the other is $m_h = 1$ and $m_v = 2$) such that the right number of lines are included in the case of having symmetry with respect to the origin.

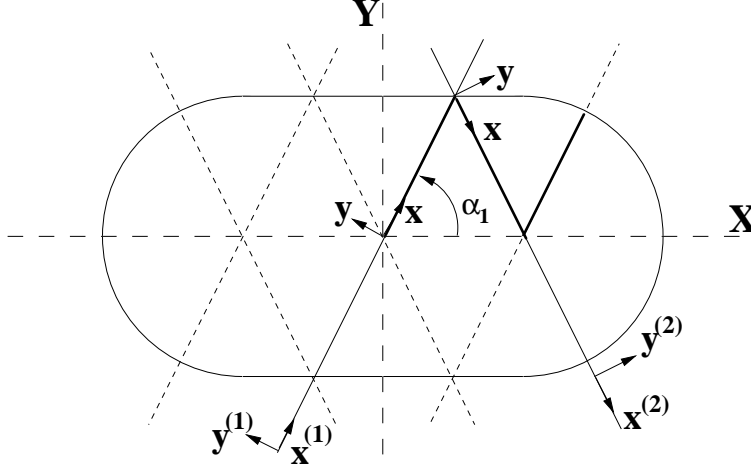


Figure 2: Set of lines including symmetries employed in the construction of resonances associated to one of the shortest periodic orbits. Different coordinate sets involved in this construction are shown.

This construction of resonances allows us to reduce calculations by exploiting the spatial symmetries of the system. We will explain the role of all these

indices and coordinate rotations. The values of the function ψ_γ in the general coordinates (X, Y) in the domain are obtained from their corresponding ones in local coordinates over each line. This is the reason why in the case of lines having no symmetry with respect to the axis X or Y , m_h and m_v adopt the value 2 in such a way that the two symmetry related lines are included (in the case of showing that symmetry, m_h and m_v have value 1 and the only line considered is the original one). Then, the values given to s_l and s_i complete this process by reflecting the corresponding coordinate. The main point about this mechanism in Eq (12) is that when second lines are involved the boundary conditions at the axes have to be met also. To achieve this result they are added with positive or negative sign if the symmetry is even (s_h or s_v equal to 0) or odd (s_h or s_v equal to 1). This can be directly verified by replacing i and l by 2 in the formulas for h_i and v_l , and also s_h and s_v by their corresponding values (always referring to the reflected lines). To satisfy the boundary conditions when a line goes through the origin of (X, Y) , only one reflection must be considered, this is the reason why this case is treated separately in our general rules of assignment for the m_h and m_v values.

Now that we have completed the construction of resonances on the domain of the billiard it is convenient to introduce the expression for the hyperbolic part of the Hamiltonian applied to these functions. As shown in Ref. [15] it has a simple form in terms of conveniently defined creation-annihilation operators and also can be expressed as:

$$\begin{aligned} \frac{(\hat{H} - E)}{\hbar^2/2M} \psi_j^{(m)} &= -\alpha(x) [\sqrt{(m+1)(m+2)} \psi_j^{(m+2)} + \\ &+ \sqrt{(m-1)m} \psi_j^{(m-2)}], \end{aligned} \quad (13)$$

with $\alpha(x) = s \, 2M\dot{x}/\hbar \, f'(x) \, \lambda/2 = s \, k \, f'(x) \, \lambda$ (where $f'(x) = 1$, s is the sign of the slope of the unstable direction with respect to the y axis at the initial point $x = x_0$, and M the mass of the particle). The case $m = 0$ corresponds to the expression given in [16]. This formula or its version on the boundary which is derived in Section 3, is the cornerstone of the short periodic orbits theory and also plays a crucial role in the construction of scar functions.

2.1 Following the phase of $Q(x)$: a local expression for resonances

We have pointed out that function $\Phi_j(x)$ is the phase accumulated by $Q(x)$ from the point $x_1 = 0$ to x over the trajectory, followed in a continuous way and incorporating jumps due to rigid walls afterwards (we isolated them by using $\tilde{M}(x)$). In this subsection we are going to explain the calculation of the continuous part in detail.

The function $\phi_j(x) = \arg[Q_j(x)] - \arg[Q_j(x_j)]$, where \arg takes the argument of a complex number in the interval $[0; 2\pi)$, follows the phase of $Q(x)$ after the bounce in x_j . We must be careful in the analysis because the phase of $Q_j(x)$ is divided by 2. Then, the proposed method will be to consider the phase of $Q_j(x)$ in an arbitrary point of the line j . The complex vectors $Q(x)$ and $P(x)$ are obtained by

$$\begin{pmatrix} Q_j(x) \\ P_j(x) \end{pmatrix} = M_1(x - x_j) \begin{pmatrix} a_j & b_j \\ c_j & d_j \end{pmatrix} \begin{pmatrix} e^{-(x-x_j)\lambda} \\ i e^{(x-x_j)\lambda} \end{pmatrix},$$

where

$$\begin{pmatrix} a_j & b_j \\ c_j & d_j \end{pmatrix} = \tilde{M}(x_j^+) B \begin{pmatrix} e^{-x_j\lambda} & 0 \\ 0 & e^{x_j\lambda} \end{pmatrix} = \begin{pmatrix} y_u(x_j) & y_s(x_j) \\ p_u(x_j) & p_s(x_j) \end{pmatrix}.$$

Here x_j^+ means (for $j \geq 2$) that \tilde{M} (the stability matrix multiplied by $(-1)^{N_b(x_j^+)}$) is evaluated after the bounce over the boundary in x_j . It can be easily verified that

$$\begin{aligned} Q_j(x) &= [a_j + (x - x_j)c_j] \exp[-\lambda(x - x_j)] + \\ &+ i[b_j + (x - x_j)d_j] \exp[\lambda(x - x_j)]. \end{aligned} \quad (14)$$

The first conclusion that we can derive from this expression is that for $x \rightarrow -\infty$, $Q(x)$ is real, with sign equal to $\text{sgn}(-c_j)$, and for $x \rightarrow +\infty$ is pure imaginary, with its sign given by $\text{sgn}(d_j)$. We will define the new variable $\tilde{x} = x - x_j$. With this definition we can easily write $Q_j(\tilde{x}) = (a_j + \tilde{x}c_j) \exp(-\lambda\tilde{x}) + i(b_j + \tilde{x}d_j) \exp(\lambda\tilde{x})$. We are going to divide the \tilde{x} axis, having in mind the places where the real and imaginary part of $Q(\tilde{x})$ change signs. These are located at $\tilde{x}_{Re} = -a_j/c_j$ for the real part and at $\tilde{x}_{Im} = -b_j/d_j$ for the imaginary one. It is easy to see that $Q(\tilde{x}_{Re})$ is pure imaginary with sign given by $\text{sgn}[(b_j c_j - a_j d_j)/c_j] = \text{sgn}(-1/c_j) = \text{sgn}(-c_j)$. On the other hand, $Q(\tilde{x}_{Im})$ is real and $\text{sgn } Q(\tilde{x}_{Im}) = \text{sgn}[(d_j a_j - b_j c_j)/d_j] = \text{sgn}(1/d_j) = \text{sgn } d_j$. Moreover, once the signs of c_j and d_j are given, the order relation between \tilde{x}_{Re} and \tilde{x}_{Im} is specified. For instance, for $c_j > 0$ and $d_j > 0$, and using the fact that $a_j d_j - b_j c_j = 1$ there results $\tilde{x}_{Re} = -a_j/c_j < -b_j/d_j = \tilde{x}_{Im}$.

The only idea that motivates the previous reasoning is the continuous evolution of $Q(\tilde{x})$, without necessarily being a monotonous one. Hence, we can have four possible sign combinations and orderings of \tilde{x}_{Re} and \tilde{x}_{Im} , as shown in Fig. 3. The same Figure also shows the evolution of $Q(\tilde{x})$ in the complex plane.

In these figures we have labelled the three sectors of the \tilde{x} axis that are defined by \tilde{x}_{Re} and \tilde{x}_{Im} with -1 , 0 and 1 . They are the three quadrants where $Q(\tilde{x})$ time evolution takes place, evolving from -1 to 0 and then to 1 . This labelling can be defined through the function:

$$n_j(\tilde{x}) = \begin{cases} 1 & \text{if } \tilde{x} > \max(-a_j/c_j, -b_j/d_j) \\ -1 & \text{if } \tilde{x} < \min(-a_j/c_j, -b_j/d_j) \\ 0 & \text{otherwise.} \end{cases}$$

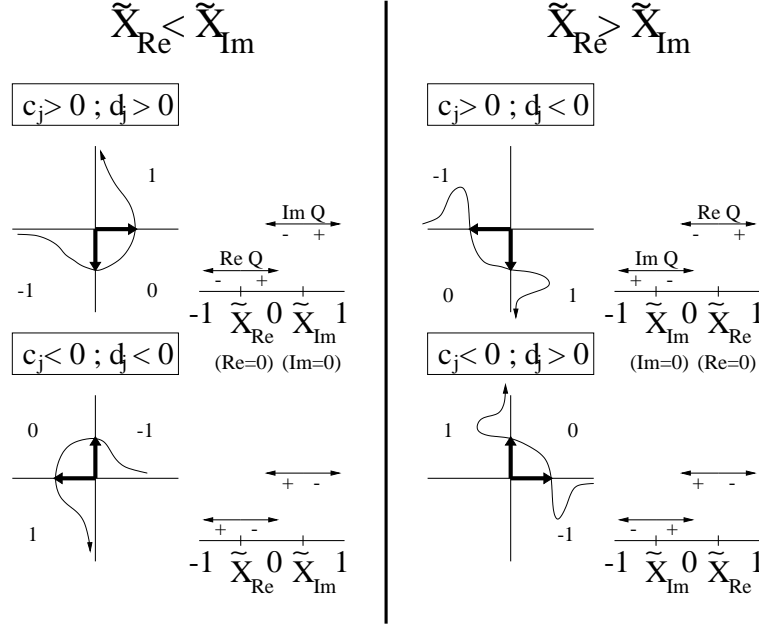


Figure 3: Detail of the possible evolutions of the complex number $Q(\tilde{x})$. The curves in three out of the four quadrants depict its time evolution. \tilde{x}_{Re} divides the \tilde{x} axis in domains with a positive or negative value of the real part of $Q(\tilde{x})$. The same applies to \tilde{x}_{Im} but for the imaginary part. Numbers -1 , 0 and 1 denote the quadrants visited (in the given order) by $Q(\tilde{x})$.

Though rather technical, introducing n_j allows us to define the resonances in a local form, and this is a very important feature of them. The curve representing $Q(\tilde{x})$ (in Fig. 3) is only qualitative and, of course, it does not imply monotony in the evolution. In the case of Figures corresponding to $\tilde{x}_{Re} > \tilde{x}_{Im}$, for instance when $d_j < 0$, the imaginary component of Q in the -1 region grows while \tilde{x} decreases in absolute value; but in some point it must begin to decrease in absolute value in order to pass through zero in a continuous way, following the signs of the quadrant. Something similar happens in the other cases for both asymptotic limits. The arrows over the real and imaginary axes in these four schemes represent $Q(\tilde{x}_{Re})$ if they are over the imaginary axis and $Q(\tilde{x}_{Im})$ if they are over the real axis.

Lets put again the analysis in terms of the x variable over the trajectory.

Not all the changes of quadrant imply a jump in the phase of $Q(x)$ given by the arg function. While it is true that *inside* of each quadrant there is *no* need of monotony, it *is* needed among the quadrants (this is a kind of discrete monotony that allows us to say that the phase of $Q(x)$ is greater in 1 than in 0, and it is greater in 0 than in -1). Lets suppose now that there has been a change of region (or quadrant). In the case of $\tilde{x} > 0$ (there has been an evolution from the point x_j) but $\phi_j(x) < 0$ (the phase of $Q(x)$ relative to the one that it had in x_j is lower), or $\tilde{x} < 0$ and $\phi_j(x) > 0$ (there has been a backward evolution but the phase grows), we are in a situation where the real positive axis has been crossed. Thus, we have to add or substract 2π , respectively, in order to continuously keep track of the phase (because if $\tilde{x} > 0$ there has been an evolution from x_j and the crossing has been in the counterclockwise or positive sense, and it is negative if $\tilde{x} < 0$). To summarize, if $n_j(x) \neq n_j(x_j)$ and $(x - x_j)\phi_j(x) < 0$ a phase $\alpha_j(x) = 2\pi \operatorname{sgn}(x - x_j)$ must be added; otherwise $\alpha_j(x) = 0$. If $c_j=0$ or $d_j=0$, x_j can be replaced by any other point over the j line, inside the desymmetrized billiard.

Finally, we can see that $\phi_j(x) + \alpha_j(x)$ defines the angle swept by $Q_j(x^{(j)})$ in a continuous way. Hence, $\tilde{\varphi}_j = \tilde{\varphi}_{j-1} + \phi_{j-1}(x_j) + \alpha_{j-1}(x_j)$ for $j \geq 2$ prevents the phase from jumping when changing from one line to the next one.

3 Resonances on the billiard boundary

In Section 2 we described the construction of resonances on the billiard domain. This is only suitable for calculations carried out in the low energy region, where these wave functions are simple. If we include longer orbits as well as higher energy families of the shortest ones we need to consider a reduction to a surface of section. Also, for calculations of matrix elements and for obtaining explicit expressions in terms of classical quantities when $\hbar \rightarrow 0$ is essential to perform this reduction. As a surface of section we can take any differentiable curve ξ with a coordinate q along it and another η orthogonal to ξ at the point q ($\eta = 0$ over the curve). Consider an orbit γ , its l crossings with this curve (taken to be at q_j ($j = 1, \dots, l$), with angles θ_j on ξ and at x_j on γ) define a number l of m th excited wave packets as the function $\psi_\gamma^{(m)}$ is considered only over ξ . This is in fact the representation of $\psi_\gamma^{(m)}$ on the section. In the case of billiards, systems that are bounded by rigid walls, we can take this boundary as the surface of section, equipped with Birkhoff coordinates, i.e., the boundary arclength q and the tangential momentum p at the bounce. The origin of q is at the point $(X, Y) = (0, R)$ and it grows in the clockwise sense. But for Dirichlet boundary conditions ψ_γ is null to order $\sqrt{\hbar}$ on this surface. Then, we can take

$$\varphi_\gamma^{(m)}(q) \equiv \frac{\partial \psi_\gamma^{(m)}}{\partial \eta}(x, y) \quad (15)$$

as the representation of $\psi_\gamma^{(m)}$ on the section. We are going to obtain the general expression for this function. In the neighbourhood of a bounce point, $\varphi_\gamma^{(m)}$ is given by the combination of 2 terms, one corresponding to the incoming path and the other to the outgoing one (see Fig. 4).

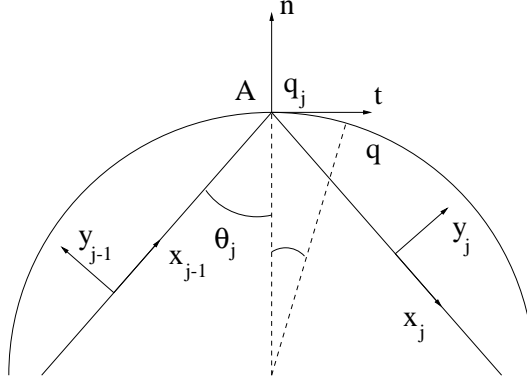


Figure 4: Incoming and outgoing paths of a given trajectory at a bounce point on the billiard boundary. Coordinates (x_{j-1}, y_{j-1}) and (x_j, y_j) on the trajectory correspond to the incoming and outgoing paths; t, n are the tangential and normal coordinates to the boundary at the bounce point A (A is the origin of x_j and n). Finally q is the arclength coordinate, with value $q = q_j$ at the j th bounce.

From this Figure we see that the normal n (the former general η coordinate specialized for this case) and tangential t coordinates can be related to the trajectory coordinates by means of simple rotations (being $x_j = \sin(\theta_j)t - \cos(\theta_j)n$, $y_j = \cos(\theta_j)t + \sin(\theta_j)n$ and $x_{j-1} = \sin(\theta_j)t + \cos(\theta_j)n$, $y_{j-1} = -\cos(\theta_j)t + \sin(\theta_j)n$). We can consider $t \simeq R((q - q_j)/R - (q - q_j)^3/(6R^3))$ for the tangential coordinate, where R is the curvature at the bounce. Also, for the normal and tangential coordinates to the boundary at the bounce point, the relation $n \simeq -t^2/(2R)$ is valid (over the boundary). For this reason we are going to take $y \simeq \cos(\theta)t \simeq \cos(\theta)(q - q_j)$ and $x \simeq \sin(\theta)(q - q_j)$ in expressions on the boundary at the lowest order in \hbar . As stated above, we can write the general expression for resonances near the j th bounce as a sum of two contributions of the type described by Eq (6), arising from the incoming and outgoing paths, respectively. We can write a real expression for the normal derivative to the lowest order in \hbar (we remember here Eq (10) and that the sin function vanishes

to order $\sqrt{\hbar}$ on the boundary):

$$\begin{aligned} \varphi_j^{(m)}(q) &= -k \cos \theta_j \left(\frac{kR}{|Q(x_j)|^2} \right)^{1/4} f^{(m)}(\xi) \\ &\quad - \frac{2}{\sqrt{L}} \cos [k \cos^2 \theta_j (q - q_j)^2 g_j(x_j) + k \sin \theta_j (q - q_j) + \Delta] \end{aligned} \quad (16)$$

where $f^{(m)}(\xi)$ is the same defined after Eq (10) in Section 2, but now taking $\xi = \sqrt{kR}(q - q_j) \cos \theta_j / |Q(x_j)|$ and $\Delta = kx_j - N_b(x_j^+) \pi/2 - (m + 1/2) \Phi_j(x_j) - F_0 - mG_0$.

As previously mentioned we have evaluated the expression on the boundary by means of the $\sqrt{\hbar}$ order approximation in the x and y variables, this being a linear approximation in the boundary variable q . Note that the ordering of bounces and lines is as follows: q_1 be the first bounce on the boundary of the stadium, then $j = 1$ is the outgoing line from it; this process extends up to $L/2$. It is important to mention that if two lines reach the bounce point, then an additional factor of 2 is needed in order to account for the different weight that these points have in “self-retracting orbits (librations)” with respect to turning points; in the case of rotations the overall factor can be considered part of the normalization condition.

We want to obtain expressions for resonances on the boundary of the first quarter of the billiard. Symmetry properties must be taken into account and one way to do so is by considering “contributions” coming from bounces that lie outside the first quarter of the boundary (see Fig. 5). The domain counterpart of these bounces are taken into account by Eq (12) of Section 2. In fact lines are continued outside the desymmetrised domain. But regarding boundary expressions we must explicitly introduce them. It is clear that in the semiclassical limit these contributions will tend to zero, but for finite \hbar we must add to the previous expressions the same ones but evaluated at $q'_j = -q_j$; $\theta'_j = -\theta_j$ when $q_j \neq 0$, and $q'_j = L/2 - q_j$; $\theta'_j = -\theta_j$ when $q_j \neq L/4$ (see Fig. 5). The case “c” of Fig. 5 can be disregarded.

Then, by adding up all the contributions at each bounce along the trajectory we arrive at the complete expression for the resonance on the boundary. This procedure is analogous to the one devised to construct the resonance on the domain by adding all contributions coming from different paths. For completeness we are going to define the hyperbolic part of the Hamiltonian acting over a resonance on the boundary as:

$$\begin{aligned} \frac{\partial(\hat{H} - E)/(\hbar^2/2m)}{\partial n} \psi_j^{(m)}|_{\xi} &\equiv \hat{H}_{eff} \varphi_j^{(m)}(q) = \\ &-s k f'(x) \lambda [\sqrt{(m+1)(m+2)} \varphi_j^{(m+2)} + \sqrt{(m-1)m} \varphi_j^{(m-2)}], \end{aligned} \quad (17)$$

In the remaining part of this section we introduce corrections to the general expression for the resonance over the boundary at each bounce. They take into

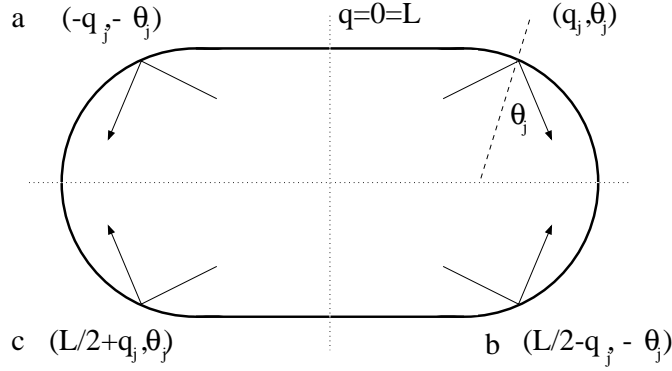


Figure 5: Horizontal and vertical symmetry related bounces and corresponding values of their Birkhoff coordinates on the stadium boundary.

account the curvature of the manifolds that is not included in the previous linear approximation. Furthermore, they apply in a direct way to the already defined expressions for the resonances and the hyperbolic Hamiltonian.

Eq (16) describes the normal derivative of the resonance on a tangential section to the boundary at a given bounce point. But this is not enough if we want to make calculations with these expressions. We therefore need to include the way manifolds depart from the unstable and stable directions given by the vectors ξ_u and ξ_s respectively. We will denote the points on the unstable (or the stable) manifold corresponding to the fixed point (q_0, p_0) by $(\tilde{q}, \tilde{p}(\tilde{q})) = (q - q_0, p - p_0)$. A description of this situation can be seen in Fig. 6. In this Figure $\tilde{p}(\tilde{q})$ is the function that defines the unstable manifold (this procedure applies equally well to the stable manifold). In the following we drop the subindex labelling the j th bounce so that making the notation easier. In order to proceed we need to change coordinates from the Birkhoff set to the ones defined by the unstable and stable directions. This task is done by the matrix \mathcal{B}^{-1} :

$$\begin{pmatrix} u(\tilde{q}) \\ s(\tilde{q}) \end{pmatrix} = \mathcal{B}^{-1} \begin{pmatrix} \tilde{q} \\ \tilde{p}(\tilde{q}) \end{pmatrix},$$

where \mathcal{B} is the matrix with columns given by the unstable and stable vectors. They are evaluated at “half a bounce” and projected on the Poincaré section. This can be obtained by means of:

$$\begin{pmatrix} 1/\cos\theta & 0 \\ 0 & \cos\theta \end{pmatrix} \begin{pmatrix} 1 & 0 \\ R/\cos\theta & 1 \end{pmatrix} \begin{pmatrix} a & b \\ c & d \end{pmatrix},$$

where the first matrix projects the vectors on the section and the second matrix stands for subtracting half a bounce to the third one on the right. In this last case, columns are the unstable and stable vectors evaluated after the considered bounce (see previous Section for details).

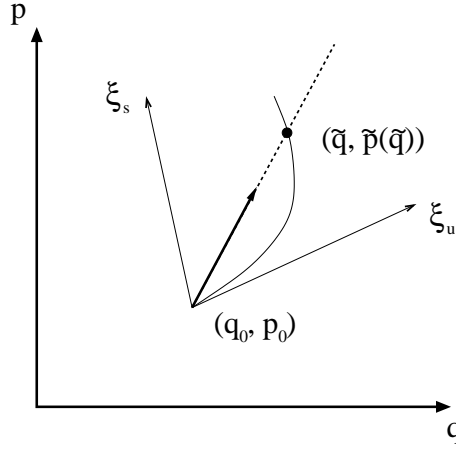


Figure 6: Description of point $(\tilde{q}, \tilde{p}(\tilde{q})) = (q - q_0, p - p_0)$ on the unstable manifold corresponding to the fixed point at (q_0, p_0) on the Poincaré section (q, p) .

With these functions at hand it is easy to see that the direction of the chord that goes through the points (q_0, p_0) and $(\tilde{q}, \tilde{p}(\tilde{q}))$ is given by the vector $\xi_u + f_u(\tilde{q})\xi_s$ with $f_u(\tilde{q}) \equiv s(\tilde{q})/u(\tilde{q}) = \alpha_u\tilde{q} + \beta_u\tilde{q}^2 + \dots$. In order to evaluate the effect on the wavefunctions this description of the manifolds should be averaged, and we propose a heuristic method to do it. A numerically verified convenient choice turns out to be the following weighted average:

$$\bar{f}_u(\tilde{q}) \equiv \int_0^{\tilde{q}} f_u(q') \frac{\tilde{q}' dq'}{\tilde{q}^2/2} = \frac{2}{3}\alpha_u\tilde{q} + \frac{1}{2}\beta_u\tilde{q}^2 + \dots \quad (18)$$

Of course, this can also be done for the function $\bar{f}_s(\tilde{q})$ which can be expanded in terms of \tilde{q} as

$$\bar{f}_s(\tilde{q}) = \frac{2}{3}\alpha_s\tilde{q} + \frac{1}{2}\beta_s\tilde{q}^2 + \dots \quad (19)$$

which gives a complete description of these second order effects. Then, the correction to the vectors $\xi_u(\tilde{q})$ and $\xi_s(\tilde{q})$ is the most direct method to include them in the resonances. The new vectors now depend on the boundary variable \tilde{q} and must satisfy also the normalization condition $\xi_u(\tilde{q}) \wedge \xi_s(\tilde{q}) = J$. In fact, the normalization factor does not play any role in the wave function since, for instance, it cancels out in $\Gamma(\tilde{q})$. Therefore, we do not show it in the following formulae for the \tilde{q} dependent unstable and stable vectors:

$$\xi_u(\tilde{q}) = (1 + \eta \bar{f}_u)[\xi_u + \bar{f}_u(\tilde{q})\xi_s], \text{ and } \xi_s(\tilde{q}) = (1 + \eta \bar{f}_s)[\xi_s + \bar{f}_s(\tilde{q})\xi_u], \quad (20)$$

where $\eta = -\text{sgn}(q_u q_s) \sin^2 \theta$. The factors $(1 + \eta \bar{f}_u)$ and $(1 + \eta \bar{f}_s)$ are due to the fact that, for high values of p , projecting the unstable and stable vectors on the Poincaré section results into a stretching of them in q direction and a contraction in p . Then, when modified to consider nonlinear effects by means of $\bar{f}_u(\tilde{q})$ and $\bar{f}_s(\tilde{q})$, a similar definition for both vectors is guaranteed by this factor. Finally, the way in which all this corrections enter the previous expressions is by new versions of $Re[P(\tilde{q})/Q(\tilde{q})]$ and $\phi(\tilde{q})$ expanded in powers of \tilde{q} . It is worth to mention that these Q and P are different from those obtained in the previous section, the new ones are on the surface of section. Then, the final expressions can be obtained by taking into account that now, for instance, $Q = (q_u + \bar{f}_u(\tilde{q}) q_s) (1 + \eta \bar{f}_u(\tilde{q})) + i (q_s + \bar{f}_s(\tilde{q}) q_u) (1 + \eta \bar{f}_s(\tilde{q}))$ and equivalently for P . Then, it is easy to see that

$$\tilde{g}(\tilde{q}) = Re \left(\frac{P}{2Q}(\tilde{q}) \right) = \frac{p_u q_u + p_s q_s}{2(q_u^2 + q_s^2)} + \frac{g_q R \tilde{q}}{3(q_u^2 + q_s^2)^2} + \mathcal{O}(\tilde{q}^2), \quad (21)$$

with $g_q = (\alpha_u + \alpha_s)(q_u^2 - q_s^2) + 2(\alpha_u - \alpha_s)|q_u q_s| \sin^2 \theta$, and where the \tilde{q} independent part can be related to the expression for $g(x)$ given previously (see Section 2). In that case expressions were valid in the domain but here they are given on the boundary (notice the different coordinate dependence). Finally,

$$\tilde{\phi} = \phi + \frac{2}{3}[(\alpha_s q_u^2 - \alpha_u q_s^2) + (\alpha_u - \alpha_s)|q_u q_s| \sin^2 \theta] \frac{\tilde{q}}{q_u^2 + q_s^2} + \mathcal{O}(\tilde{q}^2). \quad (22)$$

Then, the expression for the resonance on the boundary (at each bounce) becomes:

$$\begin{aligned} \varphi^{(m)}(\tilde{q}) &= -k \cos \theta \left(\frac{kR}{|Q_0|^2} \right)^{1/4} f^{(m)}(\xi) \\ &\quad \frac{2}{\sqrt{L}} \cos[k\tilde{g}(\tilde{q})\tilde{q}^2 + k \sin(\theta)\tilde{q} + \tilde{\Delta}] \end{aligned} \quad (23)$$

with $\tilde{\Delta}$ the same as in Eq (16) but taking $\tilde{\phi}$ in place of ϕ in the expression for Φ . As can be seen we have corrected the phase only since the amplitude corrections are not relevant. To summarise, we have modified the vectors ξ_u and ξ_s in order to take into account the effect of the curvature of the manifolds in the resonances on the boundary. Our approach allows us to keep the expressions in their compact fashion.

3.1 Scar function: from the domain to the boundary

Now that we have obtained a basis of resonances expressed on the billiard boundary for a given trajectory γ and for a quantized energy E_γ (Eq (23)), we can translate this to the scar functions. They are linear combinations of resonances having the form [15]:

$$\phi_\gamma = \sum_{j=0}^N c_j \psi_\gamma^{(4j)} / \sqrt{\sum_{j=0}^N c_j^2}, \quad (24)$$

with minimum dispersion σ , where

$$\sigma^2 \equiv \langle \phi_\gamma | (\hat{H} - E_\gamma)^2 | \phi_\gamma \rangle = \langle \phi_\gamma | \hat{H}_h^2 | \phi_\gamma \rangle. \quad (25)$$

The boundary representation only amounts to take the normal derivative in each term in the previous sum. Also, the second order corrections enter immediately through each resonance. We illustrate this by means of Figs. 7 and 8, where several examples of short periodic orbits and linear density plots of the Husimi distributions of the corresponding scar functions are displayed. In this latter case the solid lines that pass through each fixed point on the Poincaré section represent the unstable and stable manifolds. Finally, the relevance of the new formulation can be appreciated with the aid of Fig. 9, where the scar function in the linear approximation can be observed, in this case the one corresponding to orbit 2 (see Fig. 7 for reference).

For comparison purposes, we would like to show the scar functions on the domain also. The same set of orbits is used for constructing them. They can be seen in Figure 10.

4 Conclusions

Resonances on periodic orbits form a convenient basis for the investigation of chaotic eigenfunctions. In the present paper we have extended the construction of resonances without excitations in the Bunimovich stadium billiard domain to resonances with transversal excitations and also to scar functions. A detailed explanation is given, providing an explicit local expression for these wave functions. We have also extended the construction of resonances and scar functions from the domain to the boundary of this billiard. This procedure enables different sorts of applications, the most remarkable one being the possibility to extend calculations of eigenstates (in the context of the semiclassical theory of short periodic orbits [16, 17]) well above the first low-lying ones. In principle this task could have been carried out on the domain also, but it would have been very demanding in terms of numerical effort and practically turns out to be impossible. The construction of resonances and scar functions on the boundary is one of the main results of this paper.

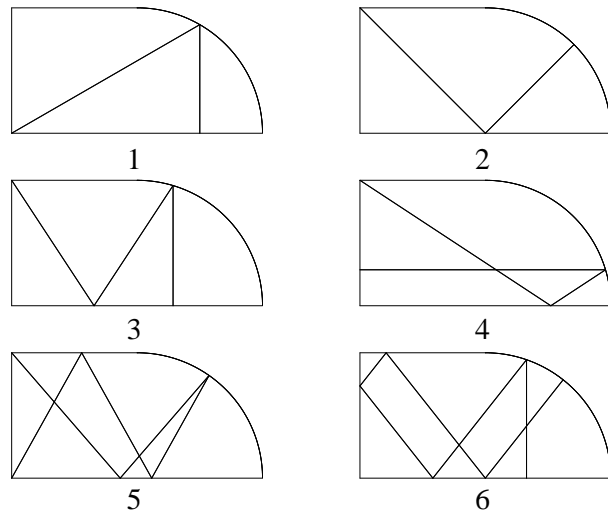


Figure 7: Some of the shortest periodic orbits of the (desymmetrised) Bunimovich stadium billiard.

We have also accounted for the departure of the unstable and stable manifolds from the linear regime, which is the other important main result of the present work. The departure is reflected in modified expressions for the resonances and scar functions. The developed method is of general scope and not only can be applied to general systems but also to any kind of non linear behaviour of the unstable and stable manifolds. This is important to underline, since the previous construction of resonances was related only to the linear motion around the trajectories, and its area of approximate validity shrinks as the energy grows. With the improved but still compact expressions for the resonances and scar functions we are able to work with a constant effective area.

Moreover, the direct geometrical approach involved in accounting for second order effects due to the projection on the boundary Poincaré section makes the expressions extremely suitable for calculations. A deep exploration of a great number of highly excited eigenfunctions arises as a realistic possibility due to the improved speed inherent to one dimensional calculations. This will allow us to study large sets of eigenfunctions and evaluate statistical measures.

Finally, with these expressions several integrals made on the domain will turn out to be one dimensional Gaussian integrals now, simplifying the theoretical analyses.

Acknowledgments

This work was partially supported by SECYT-ECOS. We are grateful to Henning Schomerus for his helpful suggestions on the original manuscript.

References

- [1] Berry M V 1977 *J. Phys. A: Math. Gen.* **10** 2083
- [2] Voros A 1979 *Stochastic Behaviour in Classical and Quantum Hamiltonian Systems* ed G. Casati and G. Ford (Berlin: Springer)
- [3] Shnirelman A I 1974 *Usp. Mat. Nauk.* **29** 181
- [4] Colin de Verdière Y 1985 *Commun. Math. Phys.* **102** 497
- [5] Heller E J 1984 *Phys. Rev. Lett.* **53** 1515
- [6] Bunimovich L A 1979 *Comm. Math. Phys.* **65** 295
- [7] Bogomolny E B 1988 *Physica D* **31** 169
Berry M V 1989 *Proc. R. Soc. London A* **423** 219
- [8] Kudrolli A, Kidambi V and Sridhar S 1995 *Phys. Rev. Lett.* **75** 822
- [9] Fromhold T M *et al.* 1995 *Phys. Rev. Lett.* **75** 1142
Wilkinson P B 1996 *et al. Nature* **380** 608
- [10] Wintgen D and Friedrich H 1986 *Phys. Rev. Lett.* **57** 571
Du M L and Delos J B 1987 *ibid.* **58** 1731
- [11] Main J, Wiebusch G, Holle A and Welge K H 1986 *Phys. Rev. Lett.* **57** 2789
- [12] de Polavieja G G, Borondo F and Benito R M 1994, *Phys. Rev. Lett.* **76** 1613
Wisniacki D A, Borondo F, Vergini E and Benito R 2001 *Phys. Rev. E* **59** 6609
- [13] Kaplan L and Heller E J 1999 *Phys. Rev. E* **59** 6609
Kaplan L and Heller E J 2001 *Phys. Rev. E* **63** 066220
- [14] Tomsovic S and Heller E J 1993 *Phys. Rev. Lett.* **70** 1405
Tomsovic S and Lefebvre J H 1997 *Phys. Rev. Lett.* **79** 3629
- [15] Vergini E G and Carlo G G 2001 *J. Phys. A* **34** 4525
- [16] Vergini E G 2000 *J. Phys. A* **33** 4709

- [17] Vergini E G and Carlo G G 2000 *J. Phys. A* **33** 4717
- [18] Yakubovich V A and Starzhinskii V M 1975 *Lineal Differential Equations with Periodic Coefficients* (New York: Wiley)

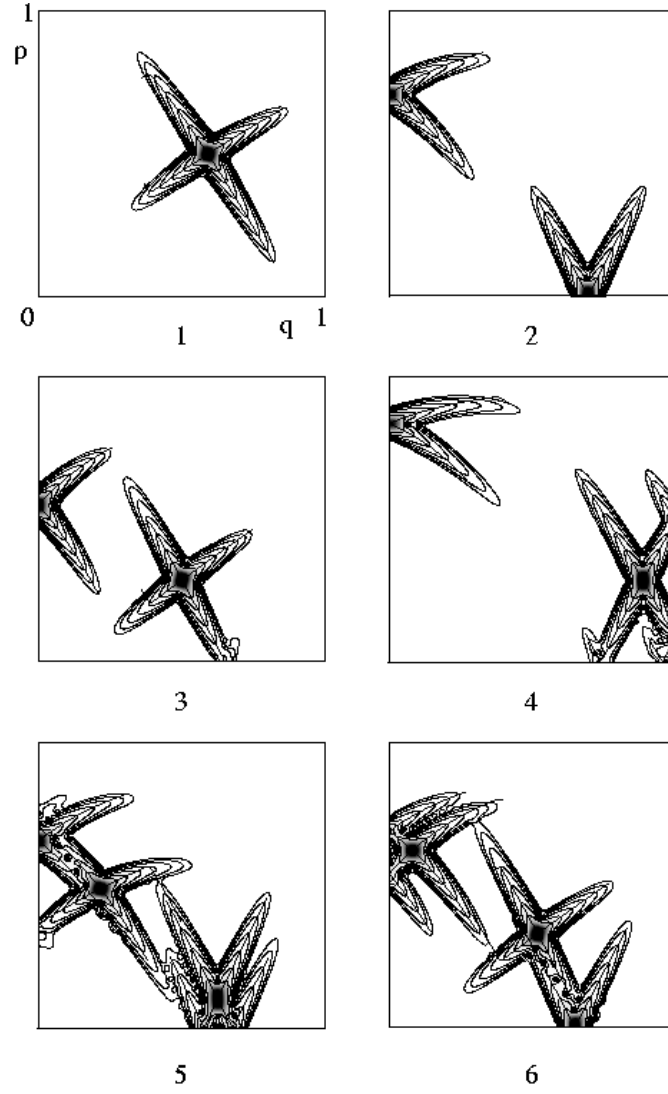


Figure 8: Linear density and logarithmic contour plots of Husimi distributions for the even scar functions corresponding to the orbits displayed in Figure 7 (numbers below them are the same as for the orbits). A logarithmic scale of uniform level ratio $1/e$ from the maximum downwards was used in the contour plots. Different levels of gray, uniformly distributed, complete this picture. Solid lines passing through fixed points represent the unstable and stable manifolds. The wavenumbers are the nearest to 1000 allowed by the quantisation conditions.

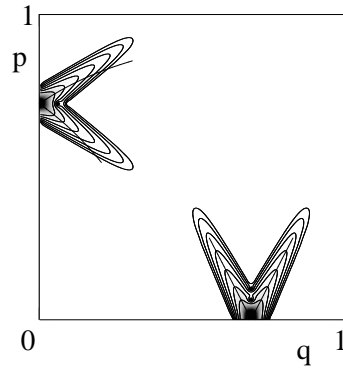


Figure 9: Linear density and logarithmic contour plot of the Husimi distribution for the even scar function corresponding to orbit 2 displayed in Figure 7. The same scales and details of Fig. 8 have been considered here.

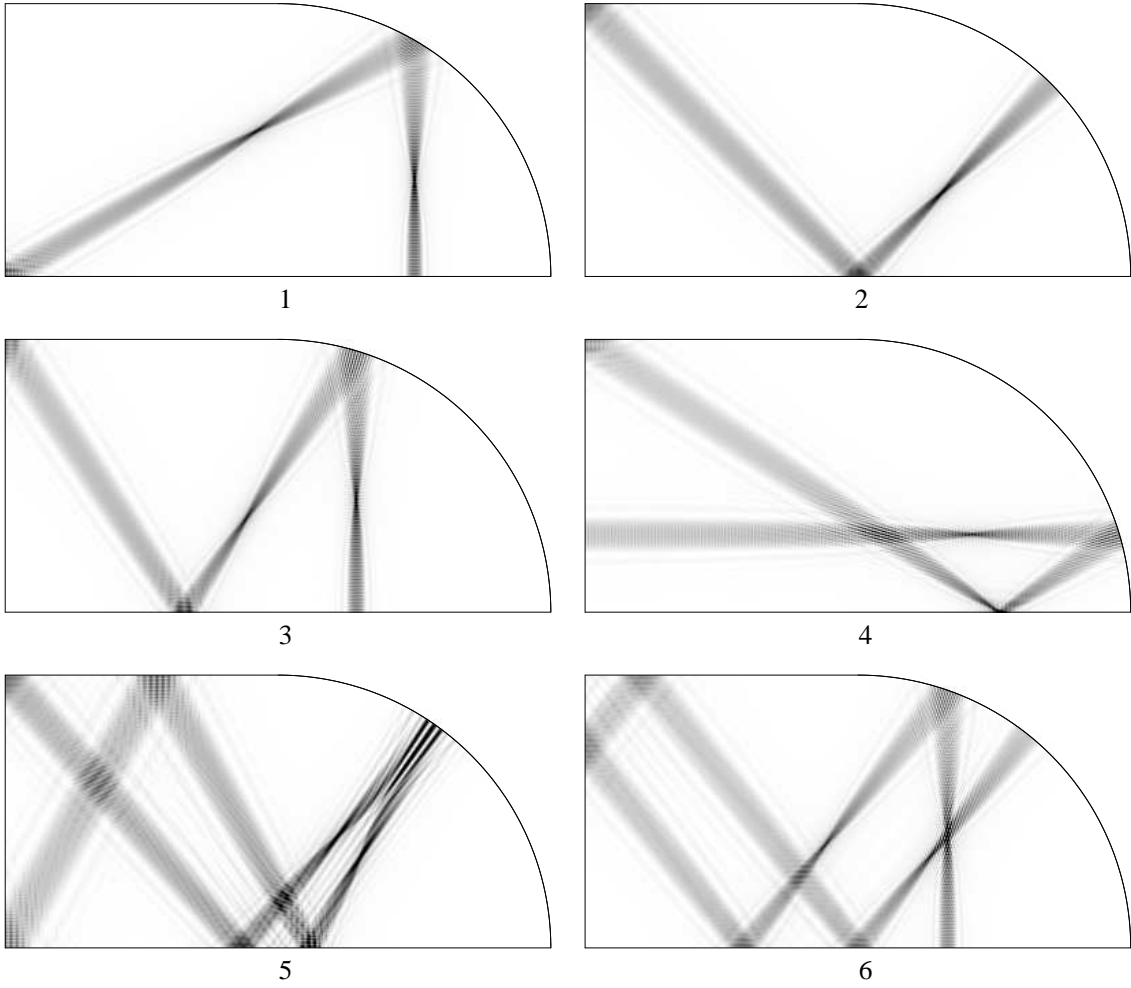


Figure 10: Linear density plots of the scar functions of Figure 8 on the domain of the desymmetrised stadium billiard.